IEEE Access
Multidisciplinary | Rapid Review | Open Access Journal

Received March 26, 2020, accepted April 7, 2020, date of publication April 20, 2020, date of current version May 12, 2020.

*Digital Object Identifier 10.1109/ACCESS.2020.2988709*

# Shielding Effectiveness Analysis of the Conducting Spherical Shell With a Circular Aperture Against Low Frequency Magnetic Fields

**XIAOCHEN YANG[1], ZHIXIN ZHANG[1], FENG NING[1], CHONGQING JIAO[1], AND LONGLONG CHEN[2]**

[1]State Key Laboratory of Alternate Electrical Power System With Renewable Energy Source, North China Electric Power University, Beijing 102206, China
[2]State Key Laboratory of Advanced Power Transmission Technology, Global Energy Interconnection Research Institute, Beijing 102200, China

Corresponding author: Chongqing Jiao (cqjiao@ncepu.edu.cn)

This work was supported in part by the Open Research Fund of the State Key Laboratory of Advanced Power Transmission Technology under Grant GEIRI-SKL-2018-006, and in part by the Fundamental Research Funds for the Central Universities under Grant 2019MS003.

**ABSTRACT** In this paper, an analytical model is presented to calculate the low frequency magnetic shielding effective (SE) of the spherical shell with a circular aperture and finite conductivity. This model is obtained by the combination of two submodels: the finite conductivity shell without the aperture, and the perfect conductor shell with the aperture. Both the submodels have existing analytical solutions. The first submodel represents the diffusion effect of magnetic field penetration through the conducting shell, and the second one denotes the aperture effect of magnetic field leakage through the aperture. The total magnetic field is the superposition of these from the two submodels. Calculation results are provided for an aluminum spherical shell of radius 0.1m for frequencies between 10Hz and 1MHz. The results are in good agreement with these form 2D axisymmetric finite element simulations. It is shown that there is a critical frequency. Below this frequency, the diffusion effect is dominant and the SE enhances with the increase of frequency. Above this frequency, the aperture effect is dominant and the SE keeps unchanged with the variation of frequency. In addition, the phase shift characteristics are also analyzed for the two effects respectively, and are employed to elucidate the mechanism of the resonance phenomenon of the SE around the critical frequency. Further, the effect of aperture depth is investigated numerically, which shows that increasing the depth has similar effect on SE like reducing aperture radius.

**INDEX TERMS** Shielding effectiveness, spherical shield, a circular aperture, the resonance phenomenon, magnetic shielding.

## I. INTRODUCTION

Low frequency magnetic shielding has wide applications in many fields, like electric vehicles [1], [2], wireless power transmission (WPT) system [3]–[5], ultrasensitive atomic sensors [6], and control circuit boards of IGBT devices [7]. Usually, a metallic shell is employed as shielding enclosure. For the complete shield without openings, there are known analytical solutions for few simple configurations such as spherical shell [8], infinite cylindrical shell [8], [9] or infinite plate [10].

Frequently, there are some apertures or slots on a shielding enclosure for ventilation or cabling purposes, which can reduce the shielding effectiveness (SE). For shields with openings, usually numerical techniques are needed to analyze the shielding performance [1], [2].

This paper aims to provide a case of shields with openings which can be treated analytically: a spherical shell with a circular aperture. This geometry can be divided into two canonical problems with analytical solutions: closed spherical shell with real conductivity and perfect electric conductor (PEC) spherical shell with an aperture. The first problem corresponds to the magnetic diffusion effect in conductor, and its analytical solution is well known [8]. The second problem is related to the aperture effect of magnetic leakage, and its solution had been reported in [11], [12] under the quasi-static frame. [13]–[16] also studies electromagnetic scattering or penetration of spherical shells with aperture, but in

The associate editor coordinating the review of this manuscript and approving it for publication was Amedeo Andreotti.

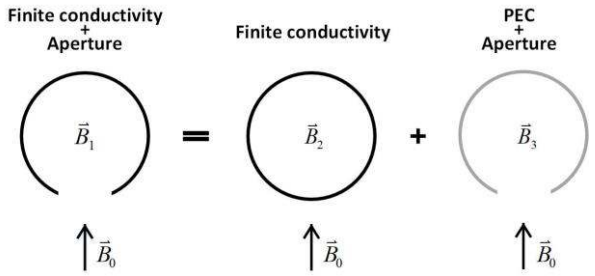


**FIGURE 1.** A finite-conductivity spherical shell with a circular aperture is divided into two submodels: a closed finite-conductivity shell and a PEC shell with aperture remained.

these studies the shell was assumed to be perfectly conducting and infinitesimally thin, and was illuminated by a plane wave. It should be noted that the idea of replacing a real shield with aperture by using two sub-models is not new. At least, this idea had been used in [1]. Nevertheless, we think that the present work is desirable because it is an infrequent analytical case which can be applied to elucidate the two magnetic shielding effect with clear physical significance. Especially, the low frequency resonance phenomenon observed in the transition region of the two effect can be explained very well. It should also be noted that the low frequency resonance phenomenon had been analyzed in earlier work [17], [18], where the shields were metallic boxes with seams, which can not be dealt with analytically. In fact, in [17] experimental data had been used to separate the contributions from the two effects, and in [18] the aperture effect was only contained in the experimental results but can not be treated by the numerical model.

This paper is organized as follows. Section II introduces the analytical model. In section III, the validation of the model is verified by comparison with finite element simulations, and its feasibility to larger aperture is discussed in section IV. Section V pays attention to the mechanism low frequency resonance phenomenon. In addition, the influence of the aperture depth on shielding effectiveness is analyzed numerically in section VI. Finally, the conclusions are summarized in section VII.

## II. THE ANALYTIC MODEL

Fig.1 shows a conducting spherical shell with a circular aperture in the bottom. An applied magnetic field with magnetic flux density $\vec{B}_0$ is perpendicular to the aperture, and the field inside the shell is denoted by $\vec{B}_1$. For the two submodels, the field inside the shell are represented by $\vec{B}_2$ and $\vec{B}_3$, respectively. Wherein, $\vec{B}_2$ and $\vec{B}_3$ are considered to be due to the diffusion effect and aperture effect, respectively. In the following, we assume that $\vec{B}_1$ is the sum of $\vec{B}_2$ and $\vec{B}_3$: $\vec{B}_1 = \vec{B}_2 + \vec{B}_3$.

SE is defined as

$$\mathrm{SE}_1 = 20\log_{10}|B_0/B_1|\ (\mathrm{dB}) \tag{1}$$

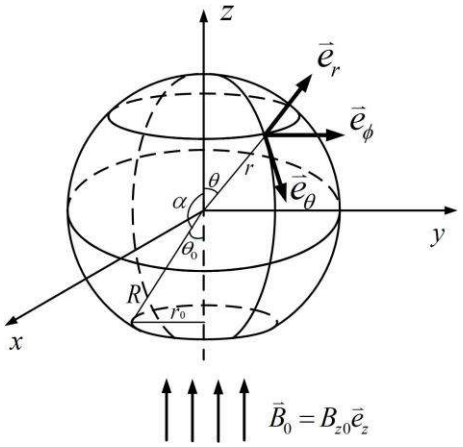


**FIGURE 2.** The spherical shield with a circular aperture.

$$\mathrm{SE}_2 = 20\log_{10}|B_0/B_2|\ (\mathrm{dB}) \tag{2}$$

$$\mathrm{SE}_3 = 20\log_{10}|B_0/B_3|\ (\mathrm{dB}) \tag{3}$$

Some information on the dimensions and coordinate of the shell is displayed in Fig. 2. The spherical shield with radius $R$ and thickness $\Delta$ is made of material with conductivity $\sigma$, relative permeability $\mu_r$ and permittivity $\varepsilon$. The circular aperture has a radius of $r_0$ and circumferential angle of $\theta_0$. The applied uniform magnetic field $\vec{B}_0$ pointing along the $z$ direction has a frequency of $f$.

The diffusion effect field $B_2$ can be written exactly as [8]

$$\begin{aligned}\frac{B_0}{B_2} &= \frac{\cosh(\gamma\Delta)}{3R^3\gamma^2\mu_r}[3R^3\gamma^2\mu_r - \Delta(\mu_r-1)(R^2\gamma^2 - 2\mu_r - 1)] \\ &+ \frac{\sinh(\gamma\Delta)}{3R^3\gamma^3\mu_r}\{R^4\gamma^4 + \gamma^2[R^2(2\mu_r^2+1) + R\Delta(3\mu_r-1)] \\ &- \mu_r^2[\Delta^2\gamma^2 + 2] + \mu_r + 1\}\end{aligned} \tag{4}$$

wherein, $\gamma \approx \sqrt{j\omega\mu_0\mu_r\sigma} = (1+j)/\delta$ is the propagation constant with $\delta = 1/\sqrt{\pi f\mu_0\mu_r\sigma}$ is the skin depth.

For the second submodel, [11] shows the magnetic vector potential inside the shell can be expressed accurately as

$$\vec{A} = A_\phi\vec{e}_\phi = \left(\frac{B_0 r}{2}\sin\theta - \frac{B_0 R}{2}\sum_{n=1}^{\infty} a_n\left(\frac{r}{R}\right)^n P_n^1(\cos\theta)\right)\vec{e}_\phi \tag{5}$$

wherein, $P_n^m(x)$ is the first kind of the associated Legendre function of degree $n$ and order $m$, and $a_n$ is expressed as

$$\begin{aligned}a_n = &\frac{-\sin(n-1)\alpha}{\pi n(n-1)} - \frac{\sin n\alpha}{\pi n(n+1)} + \frac{\sin(n+1)\alpha}{\pi n(n+1)} \\ &+ \frac{\sin(n+2)\alpha}{\pi(n+1)(n+2)}\end{aligned} \tag{6}$$

In Eq. 6, $\alpha = \pi - \theta_0 = \pi - \arcsin(r_0/R)$.

Then, we deduce $\vec{B}_3$ by solving the curl of the vector potential.

$$\frac{\vec{B}_3}{B_0} = \vec{e}_r \left[ \cos\theta - \frac{1}{2}\sum_{n=1}^{\infty} a_n \left(\frac{r}{R}\right)^{n-1} \left( -2\cos\theta P_n^{(1)}(\cos\theta) + P_n^2(\cos\theta) \right) \right] - \vec{e}_\theta \left[ \sin\theta - \frac{1}{2}\sum_{n=1}^{\infty} a_n (n+1) \left(\frac{r}{R}\right)^{n-1} P_n^1(\cos\theta) \right] \tag{7}$$

The field on the $z$-axis can be simplified into:

$$\frac{B_3}{B_0} = \vec{e}_r \left[ 1 + \sum_{n=1}^{\infty} a_n \left(\frac{z}{R}\right)^{n-1} P_n^{(1)}(1) \right] \tag{8}$$

where, $z$ is the value of the $z$-axis coordinate of the field point. Now let $z/R = q$, and using the recurrence formula:

$$xP_n^{(1)}(x) = P_{n-1}^{(1)}(x) + nP_n(x) \tag{9}$$

We get the field distribution along $z$-axis is

$$\frac{B_3}{B_0} = \frac{1}{\pi}\left( \theta_0 - \frac{q - q^{-2} + (1 - q^{-1})\cos\theta_0}{1 + q^2 + 2q\cos\theta} \sin\theta_0 - (1 + q^{-3})\arctan\left( \frac{q\sin\theta_0}{1 + q\cos\theta_0} \right) \right) \tag{10}$$

At the center of the spherical shell, Eq. 10 is simplified into

$$\frac{B_3}{B_0} = \frac{1}{\pi}\left( \theta_0 - \frac{1}{2}\sin\theta_0 - \frac{1}{2}\sin 2\theta_0 + \frac{1}{6}\sin 3\theta_0 \right) \tag{11}$$

## III. THE VALIDATION OF MODEL

Firstly, the aperture effect model is compared with the COMSOL 2D-axissymmetry FEM simulation. Tab. 1 illuminates the results for $R = 0.1$m, $\Delta = 0.3$mm with several different values of $r_0$. Where, three field points at the bottom, the center and the top of the shell, respectively, are considered. It is shown that the error between the formula solutions and the FEM solutions is less than 1%. It can be seen from Fig. 3, the shielding effectiveness increases gradually along the positive direction of the z-axis. That is, the leakage field will attenuates with the field point moving far from the aperture.

Next, all the three SEs defined in Eqs.1-3 are calculated and are compared with FEM solutions. Fig. 4 shows the dependence of SEs on the frequency for different aperture radius, thickness, and field point position. The material of the shell is aluminum with conductivity $\sigma$ =3.774 × $10^7$(S/m) and relative permeability $\mu_r = 1$. Where the black straight line, short dash line and short dot line denote the values of SE1, SE2, and SE3 obtained from FEM simulations, respectively. The red lines labelled with SE1', SE2', and SE3' refer to the analytical solutions calculated with Eq.1-3, respectively.

Taking Fig. 4(a) as an example, the frequency of the intersection of $SE_2$ curve and $SE_3$ curve is about $f_0 = 33.19$kHz. When $f < f_0$, the curve of $SE_1$ basically coincides with $SE_2$ and the penetration of magnetic field through metal is much greater than that through the aperture. When $f > f_0$, the curve of $SE_1$ is consistent with $SE_3$ and the aperture leakage effect is dominant.

There is a transition region near the critical frequency $f_0$, where the two effects have approximately equal contribution for the magnetic field. Especially, the curve of $SE_1$ contains a tip shape as shown in Fig. 4(a), which was called low frequency resonant phenomenon in [11], [18].

**TABLE 1. SE date of PEC sphere shield for several different aperture radius and field point.**

| Model Size | | SE(dB) | | |
|---|---|---|---|---|
| $R$=0.1m,Δ=0.3mm | | formula solution | FEM simulation | △SE(dB) |
| $r_0$(cm) | $z$(cm) | | | |
| 3 | 3 | 87.7856167 | 88.288 | 0.502383301 |
| | 0 | 75.77638837 | 76.215 | 0.438611627 |
| | -3 | 61.78746114 | 62.162 | 0.374538856 |
| 4 | 4 | 78.62038099 | 79.007 | 0.38661901 |
| | 0 | 62.9220612 | 63.236 | 0.313938796 |
| | -4 | 44.37756181 | 44.567 | 0.189438186 |
| 5 | 5 | 72.08301434 | 72.385 | 0.301985665 |
| | 0 | 52.73295483 | 52.949 | 0.216045171 |
| | -5 | 30.55065282 | 30.657 | 0.106347176 |

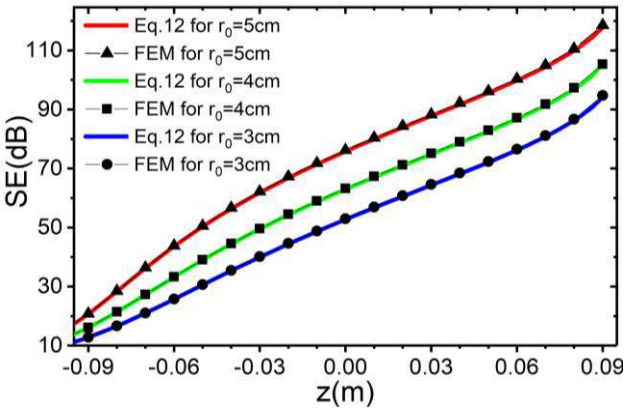


**FIGURE 3. Shielding effectiveness of PEC spherical shield versus field point position along z-axis for different values of aperture radius.**

## IV. THE EFFECT OF LARGER APERTURE SIZE

The feasibility of the present model for larger aperture size is discussed in this section. Fig. 5 displays the dependence of the SE on frequency for $r_0/R$ increasing from 0.7 to 1. It can be seen that, for $r_0/R < 0.8$, the model still work well for the whole frequency range. When $r_0/R$ reach 0.9, the deviation occurs within the low frequency region $f$ < 100Hz and the transition region 300Hz < $f$ < 4kHz. The underlying reason is that the performance of using the first submodel to represent the real diffusion effect deteriorates with the increasing of the aperture size. However, when $f$ increases further into the high frequency region ($f$ > 4kHz), this model is in good agreement with the FEM simulation again.

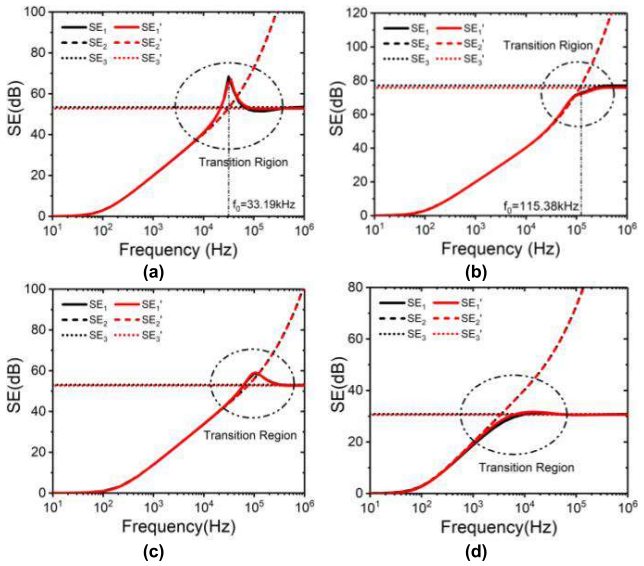


**FIGURE 4.** Shielding effectiveness curves of the aluminum spherical shield (a) $r_0 = 5$cm, $\Delta = 1$mm, $z = 0$ (b) $r_0 = 3$cm, $\Delta = 1$mm, $z = 0$ (c) $r_0 = 5$cm, $\Delta = 0.5$mm, $z = 0$ (d) $r_0 = 5$cm, $\Delta = 1$mm, $z = -5$cm.

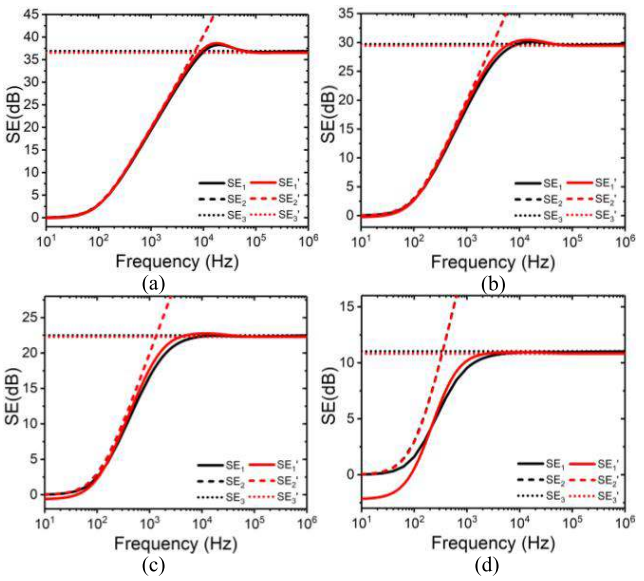


**FIGURE 5.** Shielding effectiveness versus frequency for several larger apertures (a) $r_0 = 7$cm (b) $r_0 = 8$cm (c) $r_0 = 9$cm (d) $r_0 = 10$cm.

This attributes to two aspects: in the high frequency, the skin depth is very small compared to the shell thickness and hence the conductor can be approximately treated as PEC conductor; the second submodel is feasible to any aperture size provided the material is PEC. When $r_0/R = 1$, the above tendencies observed in case of $r_0/R = 0.9$ becomes more evident. Tab. 2 lists the absolute error between $SE_1$ and $SE_1$'. We can see that the error increases with the increase of aperture size. The maximum in this table is 2.18dB, which happens at $r_0/R = 1$ and $f = 10$Hz.

**TABLE 2.** The difference between SE1 and SE1′ versus the size of the aperture.

| $r_0$ \ $f$ | 10Hz | 100Hz | 1kHz | 10kHz | 100kHz |
|---|---|---|---|---|---|
| 3cm | 0.001422 | 0.001808 | 0.000466 | 0.006579 | 0.513843 |
| 5cm | 0.019337 | 0.016742 | 0.087671 | 0.186768 | 1.189255 |
| 7cm | 0.125623 | 0.029480 | 0.384320 | 0.666047 | 0.147050 |
| 8cm | 0.283038 | 0.005368 | 0.681909 | 0.488946 | 0.079933 |
| 9cm | 0.634421 | 0.143153 | 1.046033 | 0.409945 | 0.012382 |
| 10cm | 2.177844 | 1.054353 | 0.645460 | 0.03754 | 0.138119 |

## V. THE TRANSITION REGION

There is a phase shift between the magnetic field after shielding and the applied external magnetic field. Fig. 6(a) and Fig. 6(b) show, respectively, the phase shift for the configurations in Fig. 4(a) and Fig. 4(b). The phase shift for $B_3$ is always zero, which shows that aperture leakage field is in phase with the applied field. The phase shift of $B_2$ changes with frequency, in the beginning it slowly increases from 0 to $-\pi$, and then oscillates between $-\pi$ and $\pi$. The underlying reason is that, the phase velocity of electromagnetic wave in conducting medium is very slower than that in free space and decreases gradually with the increasing frequency.

Here, we use $f_1$ to represent the frequency at which the phase shift of $B_2$ is $-\pi$. In Fig. 6(a), $f_0$ is close to $f_1$, and hence at the critical frequency $B_2$ and $B_3$ is out of phase. As a result, the two fields cancel out each other to a great extent and the total field $B_1$ becomes very small, which causes the tip in the SE curve. However, in Fig. 6(b), $f_1$(37.68kHz) is much smaller than $f_0$ (115.38kHz). At $f_0$, the phase shift of $B_2$ is about $\pi/2$ and hence the total field $B_1$ is about $2^{-1/2}$ times of $B_2$ or $B_3$. So, there is not tip existing in the SE curve.

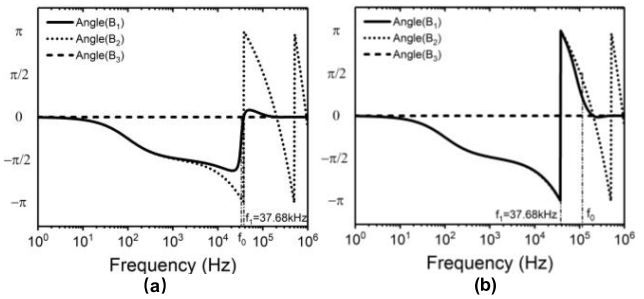


**FIGURE 6.** The phase shift versus frequency for configurations used in Fig. 4(a) and Fig. 4(b).

## VI. THE EFFECT OF THE APERTURE DEPTH

In practical engineering application, when the shield has to be perforated with a larger radius, increasing the depth of the aperture by extending it into a tube can be employed to improve the SE further. As shown in Fig. 7, the aperture depth (or the tube length) is *d,* and the thickness of the tube is same as that of the spherical shell.

Taking the case in Fig. 4(a) as an example, where $r_0 = 5$cm, $\Delta = 1$mm and the observation point is at the

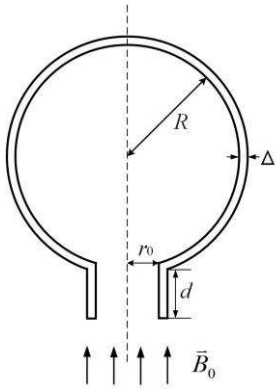


**FIGURE 7.** The spherical shield with a certain depth of circular aperture.

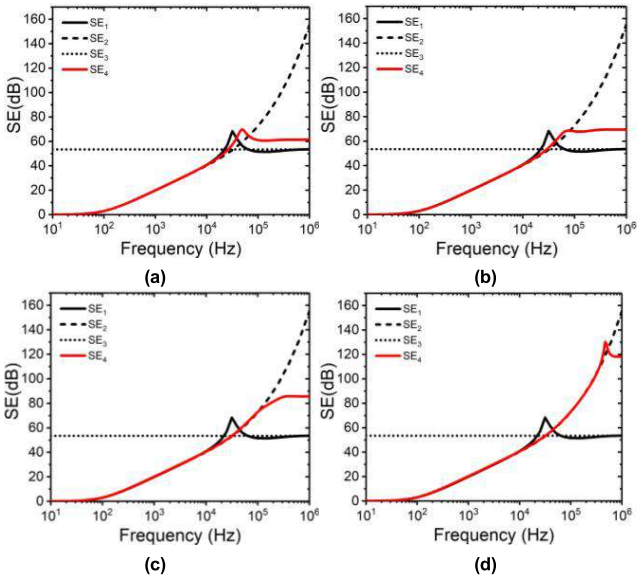


**FIGURE 8.** Dependency of the shielding effectiveness on frequency for the aluminum spherical shield with different aperture depth (a)$d/r_0 = 0.25$ (b)$d/r_0 = 0.5$ (c)$d/r_0 = 1$ (d)$d/r_0 = 2$.

center of the sphere. The SE dependency on frequency for different aperture depth are shown in Fig. 8. Meanwhile, the SE dependency on the aperture depth for four different frequencies is shown in Fig. 9. Wherein, $SE_4$ denotes the SE with aperture depth considered and is obtained from FEM simulations. $SE_1$, $SE_2$, and $SE_3$ have the same meaning aforementioned.

From Fig. 8, we can see that the critical frequency enhances with the increase of the depth. Similarly, below the critical frequency the SE follows the same trajectory like the complete shell without aperture; above the critical frequency, the SE approximately keeps unchanged with frequency variation. From Fig. 9, we can see that aperture depth up to five times the radius can not improve the SE for lower frequencies below 10 kHz. Meanwhile, $SE_4$ is nearly equal to $SE_2$ for higher frequencies. For higher frequencies above 100kHz, with the increase of the depth, the $SE_4$ (in dB) approximately

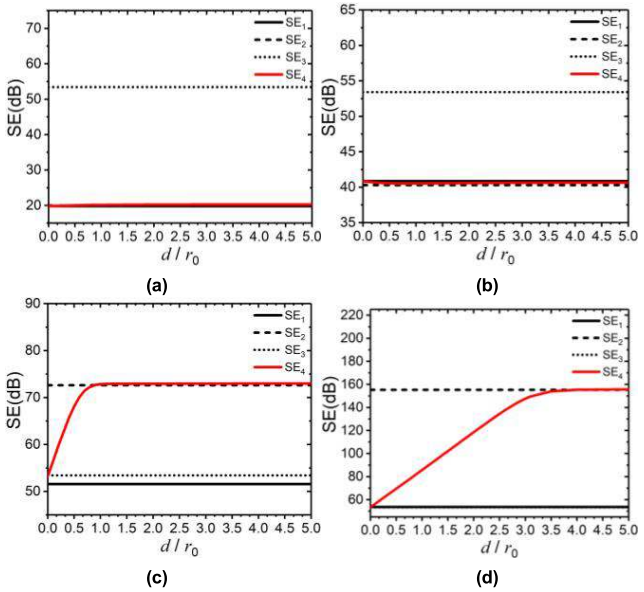


**FIGURE 9.** Dependency of the shielding effectiveness of the aluminum spherical shield on aperture depth for different frequencies (a) $f = 1$kHz (b) $f = 10$kHz (c) $f = 100$kHz (d) $f = 1$MHz.

increases linearly at first and then keeps at the constant equal to $SE_2$.

## VII. CONCLUSION

For a conducting spherical shell with a circular aperture in a uniform time harmonic magnetic field, the magnetic field inside the spherical shell can be expressed as the superposition of two analytical solutions: a spherical shell with finite conductivity without an aperture and a PEC spherical shell with a circular aperture. Compared with the results of 2D axisymmetric finite element simulations, the validation of the calculation results is verified. Taking the magnetic field direction perpendicular to the opening surface, the calculation results of the aluminum spherical shell with a circular aperture in this paper show that:

1) For the magnetic field penetrating the metal conductor into the spherical shell, its amplitude decreases with the increase of frequency, and its phase shift changes with the frequency.

2) For the magnetic field leaking into the spherical shell from the aperture, its amplitude remains unchanged and its phase shift is always zero within the considered frequency range.

3) There is a critical frequency $f_0$. Below the critical frequency, SE is mainly determined by the magnetic field penetrating the metal material, and gradually enhances with the increase of the frequency. Above the critical frequency, SE is mainly determined by the magnetic field leaked from the aperture and remains unchanged with frequency changing.

4) At the critical frequency $f_0$, the amplitude of $B_2$ and $B_3$ are equal. If the phase shift of $B_2$ at this frequency is about $-\pi$, the cancellation effect of the two fields will lead

to a significant increase in the shielding effectiveness, which is the physical mechanism of the low-frequency resonance phenomenon mentioned above.

5) The critical frequency is affected by the thickness of the spherical shell $\Delta$, the radius of the aperture $r_0$ and the observation position. When other conditions remain unchanged, $f_0$ decreases with the increase of $r_0$ or $\Delta$, and enhances with the increase of $z$.

6) With the increase of the aperture radius, the performance of the present model slightly degrades, especially for the low frequency and the transition region. In the high frequency region, the present model is always effective even when the aperture radius is up to the sphere radius.

7) By extending the aperture into a tube, the aperture depth can be increased. Then, the critical frequency can be enhanced by increasing the depth.

Finally, it is worth mentioning that the aforementioned analytical model can be extended to the case where the magnetic field is along any direction. In [11], the analytical solutions are given for two cases: the magnetic field direction is vertical and parallel to the aperture surface. Then, any direction can be considered by the superposition of the two orthogonal directions. However, for FEM simulation, 3D model is required to handle with other directions, which will consume more computer time and memory resources.

## REFERENCES


[1] A. Frikha, M. Bensetti, F. Duval, N. Benjelloun, F. Lafon, and L. Pichon, "A new methodology to predict the magnetic shielding effectiveness of enclosures at low frequency in the near field," *IEEE Trans. Magn.*, vol. 51, no. 3, pp. 1–4, Mar. 2015.

[2] A. Frikha, M. Bensetti, L. Pichon, F. Lafon, F. Duval, and N. Benjelloun, "Magnetic shielding effectiveness of enclosures in near field at low frequency for automotive applications," *IEEE Trans. Electromagn. Compat.*, vol. 57, no. 6, pp. 1481–1490, Dec. 2015.

[3] S. Lee, J. Park, K. Cho, H. Lee, C. Seo, S. Ahn, J. Kim, D.-H. Kim, Y. Cho, H. Kim, C. Song, S. Jeong, J. Song, G. Park, and S. Hong, "Low leakage electromagnetic field level and high efficiency using a novel hybrid loop-array design for wireless high power transfer system," *IEEE Trans. Ind. Electron.*, vol. 66, no. 6, pp. 4356–4367, Jun. 2019.

[4] C. Lu, X. Huang, C. Rong, Z. Hu, J. Chen, X. Tao, S. Wang, B. Wei, and M. Liu, "Shielding the magnetic field of wireless power transfer system using zero-permeability metamaterial," *J. Eng.*, vol. 2019, no. 16, pp. 1812–1815, Mar. 2019.

[5] Y. Zhou, L. Zhang, S. Xiu, and W. Hao, "Design and analysis of platform shielding for wireless charging tram," *IEEE Access*, vol. 7, pp. 129443–129451, 2019.

[6] D. Ma, M. Ding, J. Lu, H. Yao, J. Zhao, K. Yang, J. Cai, and B. Han, "Study of shielding ratio of cylindrical ferrite enclosure with gaps and holes," *IEEE Sensors J.*, vol. 19, no. 15, pp. 6085–6092, Aug. 2019.

[7] J. Zhang, T. Lu, W. Zhang, X. Bian, and X. Cui, "Characteristics and influence factors of radiated disturbance induced by IGBT switching," *IEEE Trans. Power Electron.*, vol. 34, no. 12, pp. 11833–11842, Dec. 2019.

[8] S. Celozzi, R. Araneo, and G. Lovat, *Appendix B: Magnetic Shielding*. New York, NY, USA: Wiley, 2008, pp. 282–316.

[9] Y.-P. Loh, "Shielding theory of coaxial cylindrical structures," *IEEE Trans. Electromagn. Compat.*, vol. EMC-10, no. 1, pp. 16–28, Mar. 1968.

[10] J. R. Moser, "Low-frequency shielding of a circular loop electromagnetic field source," *IEEE Trans. Electromagn. Compat.*, vol. 9, no. 1, pp. 6–18, Mar. 1967.

[11] K. Casey, "Quasi-static electric- and magnetic-field penetration of a spherical shield through a circular aperture," *IEEE Trans. Electromagn. Compat.*, vol. EMC-27, no. 1, pp. 13–17, Feb. 1985.

[12] F. M. Tesche, "Electromagnetic field shielding of a spherical shell—Revisited," *Appl. Comput. Electromagn. Soc. Newslett.*, vol. 23, no. 3, pp. 1–20, 2008.

[13] B. Enander, "Scattering by a spherical shell with a small circular aperture," *EMP Interact. Notes*, vol. 77, pp. 1–14, Aug. 1971.

[14] M. I. Sancer, and N. A. Varvatsis, "Electromagnetic penetrability of perfectly conducting bodies containing an aperture," *EMP Interact. Notes*, vol. 49, pp. 1–23, Aug. 1970.

[15] S. Chang, "Scattering by a spherical shell with a circular aperture," Dept. Commerce, Univ. Michigan, Ann Arbor, MI, USA, Tech. Rep. 5548-T-RL-2069, Jan. 1968.

[16] R. W. Ziolkowski, D. P. Marsland, L. F. Libelo, and G. E. Pisane, "Scattering from an open spherical shell having a circular aperture and enclosing a concentric dielectric sphere," *IEEE Trans. Antennas Propag.*, vol. 36, no. 7, pp. 985–999, Jul. 1988.

[17] R. Schulz, V. Plantz, and D. Brush, "Low-frequency shielding resonance," *IEEE Trans. Electromagn. Compat.*, vol. EMC-10, no. 1, pp. 7–15, Mar. 1968.

[18] W. Cooley, "Low-frequency shielding effectiveness of nonuniform enclosures," *IEEE Trans. Electromagn. Compat.*, vol. EMC-10, no. 1, pp. 34–43, Mar. 1968.


**XIAOCHEN YANG** was born in Shandong, China, in 1996. She received the B.Sc. degree in electrical engineering and automation from North China Electric Power University (NCEPU), Beijing, China, in 2018, where she is currently pursuing the M.A.Eng. degree in electrical engineering. Her research interests include electromagnetic shielding techniques and electromagnet compatibility in power systems.

**ZHIXIN ZHANG** was born in Jilin, China, in 1997. She received the B.Sc. degree in electrical engineering and automation from North China Electric Power University (NCEPU), Beijing, China, in 2019, where she is currently pursuing the M.A.Eng. degree in electrical engineering. Her research interests include electromagnetic shielding techniques and electromagnet compatibility in power systems.

**FENG NING** was born in Shanxi, China, in 1996. He received the B.Sc. degree in electrical and electronic engineering from North China Electric Power University (NCEPU), Beijing, China, in 2017, where he is currently pursuing the M.A.Eng. degree in electrical engineering. His research interests include electromagnetic shielding techniques and electromagnet compatibility in power systems.

**CHONGQING JIAO** was born in Hubei, China. He received the B.Sc. degree in geophysics from the Chinese University of Geosciences, Wuhan, China, in 2002, and the Ph.D. degree in physical electronics from the Institute of Electronics, Chinese Academy of Sciences, Beijing, China, in 2007. He is currently an Associate Professor of electrical and electronic engineering with North China Electric Power University, Beijing. His research interests include electromagnetic theory and applications and the EMC in power systems.

**LONGLONG CHEN** received the B.Sc. degree from Xi'an Jiaotong University, in 2007, and the M.Sc. degree from the Huazhong University of Science and Technology, in 2009. He is currently with the Global Energy Interconnection Research Institute. His research interests include HVDC thyristor valves, DC circuit breakers, and transmission line protection.